Review Article

PET/CT Imaging in Cancer: Current Applications and Future Directions

Michael D. Farwell, MD; Daniel A. Pryma, MD; and David A. Mankoff, MD, PhD

Positron emission tomography (PET) is a radiotracer imaging method that yields quantitative images of regional in vivo biology and biochemistry. PET, now used in conjunction with computed tomography (CT) in PET/CT devices, has had its greatest impact to date on cancer and is now an important part of oncologic clinical practice and translational cancer research. In this review of current applications and future directions for PET/CT in cancer, the authors first highlight the basic principles of PET followed by a discussion of the biochemistry and current clinical applications of the most commonly used PET imaging agent, ^{18}F-fluorodeoxyglucose (FDG). Then, emerging methods for PET imaging of other biologic processes relevant to cancer are reviewed, including cellular proliferation, tumor hypoxia, apoptosis, amino acid and cell membrane metabolism, and imaging of tumor receptors and other tumor-specific gene products. The focus of the review is on methods in current clinical practice as well as those that have been translated to patients and are currently in clinical trials. ***Cancer*** **2014;120:3433-45.** © *2014 American Cancer Society.*

KEYWORDS: cancer, positron emission tomography, fluorodeoxyglucose F18, metabolism, cell proliferation, hypoxia, protein synthesis, apoptosis.

INTRODUCTION

Conventional imaging modalities, such as plain radiography, ultrasound, computed tomography (CT), and magnetic resonance imaging (MRI), have been used for many years to identify and characterize tumors based on anatomic differences in density, water content, shape, and size. More recently, functional imaging modalities like ^{18}F-fluorodeoxyglucose-positron emission tomography (FDG-PET) have been developed that are capable of characterizing tumors based on biochemical changes at the molecular level. Since the year 2000, the number of FDG-PET scans performed in the United States has increased about 9-fold, and it is estimated that, in 2011, about 1.8 million studies were performed, and 94% of the studies were done for cancer.[1] This dramatic increase in use is likely being driven by several factors, one of which is the higher sensitivity and specificity of FDG-PET for the detection and staging of many tumors compared with anatomic imaging modalities.[2,3] In addition, PET is being used increasingly to assess therapeutic response and to characterize tumor biology. In this review, we highlight the various applications of PET imaging in cancer, including its role in personalized medicine. Although FDG continues to be the most widely used radiotracer for PET imaging (96% of PET studies in 2011 used FDG), some of the newer PET imaging agents that have been studied in humans will also be reviewed (Table 1).

Principles of PET Imaging

PET imaging uses radiopharmaceuticals labeled with positron emitting radioisotopes such as ^{11}C, ^{13}N, ^{15}O, and ^{18}F, which are produced in a cyclotron, and ^{68}Ga and ^{82}Rb, which are produced in a radioisotope generator. After a positron is emitted, it annihilates with a nearby electron and generates 2 annihilation photons (each with an energy of 511 keV), which travel in opposite directions. PET scanners are equipped with coincidence electronics to detect these pairs of photons as they hit opposing detectors nearly simultaneously. Single unpaired photons occur when one of the annihilation photons is absorbed in the body or is not detected. Although these single photons are excluded by the coincidence window, additional processes occur in PET imaging that degrade image contrast and need to be accounted for in quantitative PET imaging. Thus, various algorithms and techniques are required to correct for random coincidence events, scatter, dead-time, and various sensitivity among detectors. For accurate quantitative results, one of the most important corrections to the acquired PET image is attenuation correction. This correction is necessary because photons released from the

Corresponding author: Michael D. Farwell, MD, Division of Nuclear Medicine and Molecular Imaging, Department of Radiology, Hospital of the University of Pennsylvania, 3400 Spruce Street, Philadelphia, PA 19104; Fax: (215) 349-5843; michael.farwell@uphs.upenn.edu

Department of Radiology, Hospital of the University of Pennsylvania, Philadelphia, Pennsylvania.

DOI: 10.1002/cncr.28860, **Received:** March 14, 2014; **Revised:** May 5, 2014; **Accepted:** May 5, 2014, **Published online** June 19, 2014 in Wiley Online Library (wileyonlinelibrary.com)

center of the body, on the average, are attenuated to a greater extent than photons released from the periphery. One of the advantages of hybrid PET/CT systems is that the corresponding CT images can be used for anatomic localization as well as attenuation correction.

FDG-PET Background

FDG has its origin in the work of Sokoloff et al, who developed a method to measure regional cerebral glucose metabolism in animals using ^{14}C-deoxyglucose autoradiography.[4] Although ^{14}C-deoxyglucose is transported into cells in parallel with glucose and is phosphorylated by hexokinase to ^{14}C-deoxyglucose-6-phosphate, because it lacks a hydroxyl group at the 2 position, it is prevented from being a substrate of enzymes farther down the glycolytic pathway. Thus, ^{14}C-deoxyglucose-6-phosphate becomes trapped within cells, providing a measure of the metabolic rate. This concept was extended when FDG was developed, because FDG also lacks a hydroxyl group in the 2 position. In a similar fashion, FDG is transported into cells and phosphorylated, and it becomes trapped within cells as FDG-6-phosphate.[5] When labeled with ^{18}F, which is a positron-emitting radioisotope, FDG can be imaged with PET and used to quantify regional glucose metabolism in humans.[6]

Radiotracer uptake in PET imaging can be quantified from dynamic acquisitions performed over a period of time or from static acquisitions performed at a fixed point in time. In the research setting, dynamic imaging is often performed to measure the radiotracer uptake over time, yielding plots of radioactivity concentration versus time known as time-activity curves. Kinetic modeling can then be used, sometimes in conjunction with blood sampling, to estimate the rate of uptake and trapping of a radiotracer or to estimate the density of a receptor of interest. Because dynamic imaging is time consuming and difficult to perform over the whole body, clinical studies usually acquire a single image at approximately 60 minutes after injection of FDG. This static image is then used to calculate a simplified measure of FDG uptake, known as the standardized uptake value (SUV).[7] The SUV represents the concentration of radioactivity in the tumor tissue, normalized to the injected FDG dose and the body weight of the patient; the SUV is equal to 1 for an evenly distributed tracer. Because the SUV is typically calculated at approximately 60 minutes after injection of radiotracer, the radioactivity in metabolically active tissues is predominantly due to phosphorylated FDG rather than nonphosphorylated intracellular/intravascular FDG. Thus, the SUV is roughly proportional to the net rate of FDG phosphorylation.[8] However, SUVs are also affected by a variety of factors other than tumor glucose use; these include the time interval between injection and imaging, the size of the lesion, image reconstruction parameters, and the spatial resolution of the PET scanner. In addition, differences in the affinity and kinetics of glucose transporters and hexokinase for FDG versus glucose lead to variation in the relative trapping of each substrate in different tissues and tumors.[9] Thus, although SUVs do not provide an accurate absolute measure of tumor glucose use, they are useful for assessing interval change in metabolism, because many of the confounding issues with SUVs are negated by measuring relative change. With properly calibrated imaging devices and adherence to standard patient preparation and imaging protocols, the test-retest

TABLE 1. Overview of Current Positron Emission Tomography Radiotracers Used in Cancer Imaging

Class/Radiotracer	Target	Clinical Status
Metabolism		
^{18}F-FDG	Hexokinase	FDA approved
^{18}F-FLT	Thymidine kinase	Phase 3
^{18}F-FMAU	Thymidine kinase	Phase 1
^{18}F-ISO-1	Sigma-2	Phase 0
Hypoxia		
^{18}F-FMISO	Low oxygen	Phase 2
^{64}Cu-ATSM	Low oxygen	Phase 2
^{18}F-EF5	Low oxygen	Phase 2
^{18}F-FAZA	Low oxygen	Phase 2
^{18}F-FETA	Low oxygen	Preclinical
Apoptosis		
^{18}F/^{99m}Tc-annexin V	Phosphytidylserine	Phase 2
^{18}F-ML-10	Apoptotic changes	Phase 2
^{18}F-ICMT-11	Caspases	Phase 0
^{18}F-CP18	Caspases	Phase 0
Protein synthesis		
^{11}C-MET	Amino acid transporters	Phase 2
^{18}F-FET	Amino acid transporters	Phase 2
^{18}F-FMT	Amino acid transporters	Phase 1
^{18}F-FACBC	Amino acid transporters	Phase 2
Membrane metabolism		
^{11}C-choline	Choline kinase	FDA approved
^{18}F-choline	Choline kinase	Phase 2
Tumor-specific agents		
^{68}Ga-DOTA-TOC	Somatostatin	Phase 2
^{18}F-FES	Estrogen receptor	Phase 2
^{68}Ga-PSMA	PSMA	Phase 1

Abbreviations: ^{11}C-MET, ^{11}C-methionine; ^{64}Cu-ATSM, ^{64}Cu-diacetyl-bis(N4-methylthiosemicarbazone); ^{18}F-CP18, ^{18}F-radiolabeled pentapeptide-based substrate of caspase-3; ^{18}F-EF5, ^{18}F-radiolabeled derivative of etanidazole; ^{18}F-FACBC, 1-amino-3-^{18}F-fluorocyclobutane-1-carboxylic acid; ^{18}F-FAZA, ^{18}F-fluoroazomycin arabinoside; ^{18}F-FDG, ^{18}F-fluorodeoxyglucose; ^{18}F-FES, ^{18}F-fluoroestradiol; ^{18}F-FET, ^{18}F-fluoroethyl-tyrosine; ^{18}F-FETA, ^{18}F-fluoroetanidazole; ^{18}F-FLT, ^{18}F-fluorothymidine; ^{18}F-FMAU, 1-(2'-deoxy-2'-^{18}F-fluoro-beta-D-arabinofuranosyl)thymine; ^{18}F-FMISO, ^{18}F-fluoromisonidazole; ^{18}F-FMT, ^{18}F-fluoromethyl-tyrosine; ^{18}F-ICMT-11, ^{18}F-radiolabeled derivative of isatin; ^{18}F-ISO-1, N-(4-(6,7-dimethoxy-3,4-dihydroisoquinolin-2(1*H*)-yl)butyl)-2-(2-^{18}F-fluoroethoxy)-5-methylbenzamide; ^{18}F-ML-10, ^{18}F-radiolabeled derivative of malonic acid; ^{68}Ga-DOTA-TOC, ^{68}Ga-DOTA-Tyr^3-octreotide; ^{68}Ga-PSMA, ^{68}Ga-radiolabeled prostate-specific membrane antigen ligand; FDA, US Food and Drug Administration; PSMA, prostate-specific membrane antigen.

reproducibility of SUVs in tumors and normal tissues is high, and relative changes in SUVs as small as 20% can be used as a criterion for a metabolic response to therapy.[10,11]

The use of FDG as an agent for cancer detection is based on the observation of Warburg in the 1920s that cancer cells have abnormally high rates of glycolysis.[12] Even when tumor cells have sufficient oxygen supply, they preferentially generate energy using anaerobic glycolysis followed by metabolism of pyruvate into lactic acid.[13] In addition to elevated glycolysis, tumors often have increased expression of glucose transporters (GLUTs). These transporters allow energy-independent transport of glucose across the cell membrane down a concentration gradient. In malignant tumors, GLUT-1 is frequently overexpressed, but expression levels of GLUT-2, GLUT-3, GLUT-4, GLUT-5, and GLUT-12 also reportedly are increased in several tumors types.[14] The relative importance of GLUTs versus hexokinase activity continues to be debated, and it is likely that, in a given cell type, one may predominate.

FDG has gained widespread use in the clinic for several reasons. First, unlike glucose, FDG is excreted in the urine, which results in relatively rapid clearance of the radiotracer from the blood pool. Second, hexokinase, the target of FDG, is ubiquitous and very efficient. The net result of these 2 points is that very high target-to-background ratios are achieved by 60 minutes, with just enough background activity to enable localization of FDG-avid tumors relative to the physiologic pattern of FDG uptake. Third, there are few radiolabeled metabolites of FDG in the blood, which makes analysis of FDG uptake more straightforward. Finally, the 110-minute half-life of ^{18}F allows FDG to be produced at a central facility and transported to nearby imaging centers; thus, it is not limited to large academic centers with cyclotron facilities.

FDG-PET for Cancer Detection

FDG was first used to study tumors in the 1980s by Di Chiro, who demonstrated that the degree of malignancy of brain tumors was correlated with their FDG uptake.[15] Because FDG accumulates in most cancer cells to a greater degree than noncancer cells, FDG-PET is a very general approach to cancer imaging. Thus, FDG-PET has achieved widespread use for the detection of cancer, primarily in staging newly diagnosed or recurrent cancers. Results from the National Oncologic PET Registry, which included data from 85,658 patients with a wide variety of cancer types, concluded that FDG-PET imaging changed physicians' intended management in about 36% of patients.[16] The dominant impact was a change from nontreatment to treatment, which occurred in 29% of patients; the reverse pattern, changing from treatment to nontreatment, occurred in about 7% of patients. The types of cancer that are most commonly imaged with FDG-PET include lymphoma, head and neck cancer, lung, colorectal cancer, breast cancer, esophageal cancer, melanoma, cervical cancer, thyroid cancer, and pancreatic cancer.[17-19] Some of these cancers, such as aggressive lymphoma, squamous cell carcinoma of the head and neck, and melanoma, are usually "hot" on FDG-PET.[20] Other cancers, such as prostate cancer, neuroendocrine cancer, and well differentiated hepatocellular carcinoma, are often "cold," which limits the utility of FDG-PET in those tumors.[21,22] Still other cancers, such as breast and thyroid cancers, demonstrate a range of FDG uptake, which may be related to incompletely understood biologic factors.[23]

Recent studies have demonstrated that the activation of a variety of oncogenes results in increased FDG uptake.[24] Thus, in many patients, the degree of FDG uptake is a marker of tumor dedifferentiation. For example, when prostate cancer and thyroid cancer lose their ability to respond to androgens and trap iodine, respectively, they are much more likely to be observed with FDG-PET.[25,26] Because many factors contribute to increased FDG uptake in cancer cells, some studies have suggested that FDG-PET provides a unique measure of tumor biology that is distinct from in vitro assays.[23]

False-positive findings are relatively common on FDG-PET, because elevated glycolysis is not limited to cancer cells.[17] Typical causes of increased FDG uptake unrelated to malignancy include infectious and inflammatory etiologies, muscular activity, metabolism in brown fat, and changes in response to bone marrow-stimulating cytokines. Thus, the modest specificity and low sensitivity of FDG-PET for early stage disease limit its utility for cancer screening. However, in patients with an established diagnosis, or strong suspicion, of cancer, FDG-PET is a powerful tool that can help characterize the disease and determine its extent.

FDG-PET for Monitoring Tumor Response

It has been demonstrated that FDG-PET is useful for monitoring during treatment and assessing response after treatment has ended.[7,27,28] Many studies in breast cancer, lymphoma, lung cancer, and other tumors have demonstrated that FDG-PET can detect an early response to treatment (Fig. 1), which, in many patients, correlates well with clinical outcome, such as disease-free survival.[18,29-31] In addition, FDG-PET has been used to improve management decisions in oncologic settings. For

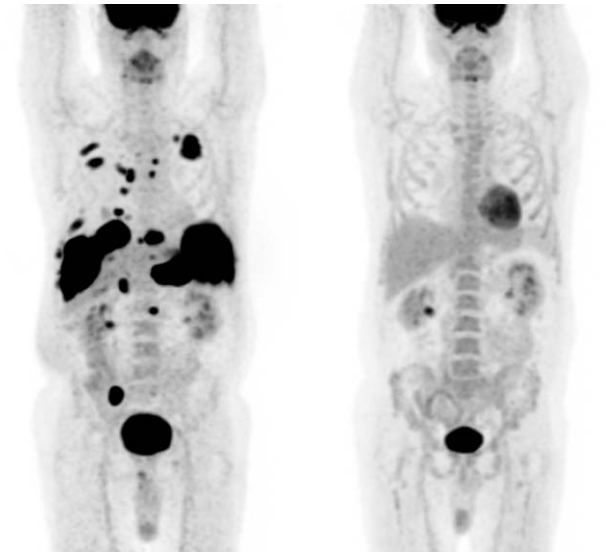

Figure 1. These are ^{18}F-fluorodeoxyglucose positron emission tomography scans from a patient with diffuse large B-cell lymphoma (*Left*) at baseline and (*Right*) 10 weeks later after 3 cycles of chemotherapy. There has been a complete metabolic response to therapy. Images are displayed in maximum intensity projection (MIP) format.

example, data from the National Oncologic PET Registry indicated that, of 10,497 treatment-monitoring PET scans performed for a wide variety of cancer types, physician-intended management changed in about 50% of patients; this included a switch to another therapy in 27% of patients, an adjustment in dose or duration of therapy in 17% of patients, and a switch from therapy to observation or supportive care in 6% of patients.[32] The expectation is that there is a strong correlation between changes in physician-intended management and patient health outcomes; however, the relationship is imperfect, and more research is needed. The goal of early monitoring for treatment response is to evaluate the effectiveness of a therapy earlier than is feasible through symptoms or other clinical parameters; ultimately, this could shorten therapeutic regimens in patients who are responding, allow for earlier changes to a new therapeutic regimen in patients who are not responding, and expedite the development of new treatments for cancer, all of which have the potential to lead to better patient outcomes.

The timing and relative change in FDG uptake during treatment appears to depend on the type of treatment used as well as the type of cancer being treated. Studies of cytotoxic chemotherapy in breast cancer, lymphoma, gastrointestinal cancers, and others indicated that FDG-PET is capable of detecting a response after a single cycle of chemotherapy.[33-35] In addition, in some lymphomas, significant changes in FDG uptake have been observed as early as 1 day after starting chemotherapy.[36] The reasons for the rapid decline in FDG uptake after cytotoxic chemotherapy are not known but are likely related to a decrease in the population of viable cells as well as a decrease in the rate of glycolysis per cell. Studies of targeted therapies like imatinib, which inhibits the c-kit growth factor pathway in gastrointestinal stromal tumors, have indicated that FDG uptake is reduced within hours of starting treatment and appears to be related to a rapid decline in glucose transporter expression.[37-39] Similarly, it has been demonstrated that the inhibition of epidermal growth factor receptor kinase by gefitinib in lung cancer cell lines results in translocation of glucose transporters from the plasma membrane to the cytosol within 4 hours.[40] However, additional studies are needed to further elucidate the mechanisms behind the rapid decline in FDG uptake in response to these classes of drugs.[41] It is noteworthy that, when treatment was temporarily held in patients with gastrointestinal stromal tumors who were taking sunitinib, a multitargeted tyrosine kinase inhibitor that also targets the c-kit pathway, many of the tumors demonstrated a rebound in FDG activity after 3 weeks, and this was followed by a decline in FDG activity when treatment resumed.[42] Thus, the finding that FDG-PET is capable of demonstrating changes in tumor biology hours to days after starting therapy gives it tremendous potential as a biomarker for tumor response to therapy, in marked contrast to conventional response measures by CT, which take weeks to months to evolve and can be misleading at early time points.[43] In most patients, successful treatment results in decreased FDG uptake; however, in certain patients, targeted therapy has resulted in increased FDG uptake at early time points during treatment. For example, a study of patients with breast cancer indicated that increased tumor FDG uptake at 7 to 10 days after the initiation of tamoxifen therapy was predictive of a subsequent clinical response.[44]

Monitoring radiotherapy with FDG-PET can be challenging, because FDG uptake is often unchanged immediately after treatment and, in some patients, may be increased.[45] The reason for this may be because, compared with chemotherapy, after radiotherapy, there is a different and longer period of viability for tumor cells or possibly a greater inflammatory response. Conversely, one study indicated that increased rather than decreased FDG uptake in high-grade gliomas after radiotherapy was predictive of a better outcome.[46]

There is no generally accepted threshold for a reduction in SUV that represents a response to treatment.

Reproducibility studies suggest that changes in SUV >20% are likely to be significant, and current guidelines recommend using a threshold of 25% or 30% for tumors with significant baseline activity.[47,48] However, the SUV thresholds used in clinical studies range from 20% to 70%, with smaller thresholds used for studies performed after a single cycle of chemotherapy and larger thresholds used for studies performed later during the course of treatment.[49] To confound matters, inflammatory tumor changes potentially can blunt the apparent reduction in SUV. For example, one study revealed that 29% of the tumor glucose use could be attributed to macrophages and granulation tissue.[50] Because different tumors and treatments result in various changes in FDG uptake, more data are needed to validate specific response criteria for FDG-PET.

FDG-PET for Prognosis

The ability of FDG to serve as a prognostic indicator in patients with cancer is incompletely understood. Intuitively, FDG uptake would be expected to reflect tumor grading, because less differentiated and more rapidly proliferating tumors should need more glucose for energy production. However, the correlation between FDG uptake and cellular proliferation, although positive, is not very strong.[24] Compared with FDG, the thymidine analog 3′-deoxy-3′-^{18}F-fluorothymidine (FLT) demonstrates a much closer correlation between uptake and labeling with Ki-67, a cellular marker of proliferation.[51] In addition, the correlation between FDG uptake and tumor grading is fairly weak for the majority of tumors; only gliomas, sarcomas, and thyroid cancers demonstrate strong correlations.[15,52,53] To make matters more complicated, some benign tumors, such as giant cell tumors, juvenile pilocytic astrocytomas, and Warthin tumors, frequently demonstrate intense FDG uptake.[54-56] Thus, although FDG uptake is modulated by several factors that often serve as poor prognostic markers, such as hypoxia, increased cellular proliferation, and the activation of a variety of oncogenes, the multifactorial etiology of increased FDG uptake limits its ability to assess for parameters other than glucose metabolism and may explain the variable success of FDG as a prognostic marker.[24]

Imaging Proliferation

Aberrantly increased cellular proliferation is a hallmark of cancer, and a decline in proliferation is one of the earliest events in response to effective cancer therapy.[57] It has been demonstrated that, in responding tumors, both chemotherapy and radiotherapy reduce proliferation rates, which precedes a reduction in tumor size.[58,59] Thus, imaging the rate of cell proliferation could permit the differentiation of benign from malignant tumors and could provide an earlier measure of therapeutic response than anatomic imaging. In addition, cell proliferation imaging has a marked advantage over anatomic imaging with regard to assessing treatment response to novel targeted agents, such as protein kinase inhibitors or antiangiogenesis agents, because some of these agents have a predominantly cytostatic effect and may not lead to rapid tumor shrinkage.

Several different radiotracers have been developed to image cell proliferation. Initial efforts focused on synthesizing analogs of thymidine, because thymidine is used by proliferating cells for DNA synthesis during the S-phase of the cell cycle but, unlike other nucleosides, is not incorporated into RNA.[60] The gold standard for assessing proliferation in vitro has long been ^{3}H-thymidine incorporation.[17] More recently, studies using ^{11}C-thymidine and PET demonstrated promise in assessing response to therapy; however, the short half-life of ^{11}C and its rapid metabolism to thymine and other metabolites made ^{11}C-thymidine impractical for routine clinical use outside of academic centers.[61] This problem spurred the development of FLT, an ^{18}F-labeled, nonmetabolized thymidine analogue that has become the most extensively studied radiotracer for imaging tumor proliferation.[62,63]

After intravenous injection, FLT enters the cell by facilitated diffusion through nucleoside transporters and is trapped in the cytosol through phosphorylation.[64] Because FLT lacks a hydroxyl group at the 3′ position, it is not incorporated into DNA, and its accumulation serves as a measure of cellular proliferation. Correlation of FLT uptake with the rate of cell proliferation in various tumor types has been demonstrated using histopathologic markers of cell proliferation, such as the Ki-67 labeling index, as the gold standard.[65] Unfortunately, most tumors demonstrate relatively low FLT uptake compared with FDG, which reduces the sensitivity of FLT-PET for detecting cancer. In addition, FLT demonstrates significant interfering physiologic activity in bone marrow and liver, and proliferating lymphocytes in reactive lymph nodes still have the potential to yield false-positive findings.[60,66] Thus, it is unlikely that FLT will have a dominant role in the initial diagnosis and staging of most cancers. Conversely, there is a general consensus that FLT-PET can be a valuable method for monitoring tumor response to treatment, especially as an early measure of response. This may be particularly important for cytostatic therapy, ie, agents that stop tumor growth but may

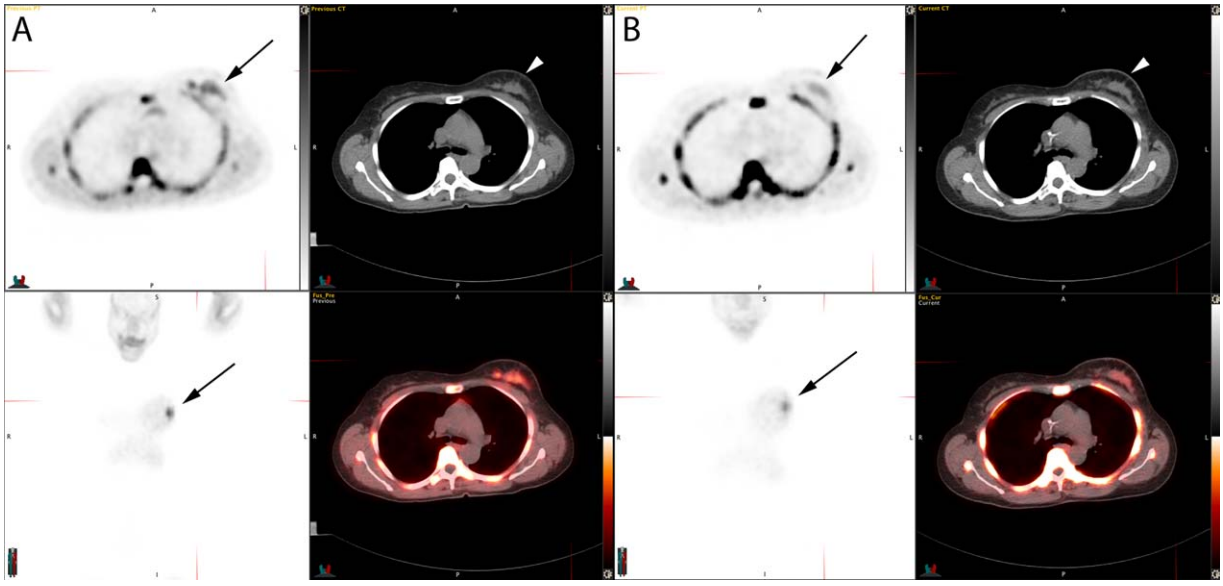

Figure 2. These are ^{18}F-fluorothymidine positron emission tomography (FLT-PET) scans from a patient with breast cancer (A) at baseline and (B) after 1 cycle of chemotherapy. Arrows indicate a breast mass in which the FLT activity has decreased over the interval, with no associated change in the size of the mass on computed tomography (CT). Axial and coronal PET images are displayed along with axial CT images and axial PET/CT fused images.

not kill tumor cells, for which proliferation imaging may play a key role in judging therapeutic effectiveness.[67]

FLT has several attractive properties as an agent for measuring cancer response. Measures of FLT uptake are precise and repeatable, with a test-retest reproducibility <10% for SUV measurements.[58] This is an important feature in using FLT-PET for serial imaging to assess response. Also, studies have indicated that changes in FLT uptake reflect changes in tumor proliferation with treatment. Preclinical work has demonstrated that a decline in FLT uptake occurs early in the course of treatment with a variety of approaches, including chemotherapy, radiotherapy, and biologically targeted agents, and several studies have noted that changes in FLT activity reflected the effects of therapy better than changes in FDG uptake.[68,69] Also, preliminary clinical studies confirmed the potential of FLT-PET for monitoring tumor response to therapy (Fig. 2). In patients with recurrent malignant brain neoplasms, tumor response assessed by kinetic measures of FLT uptake after 1 or 2 weeks of treatment with irinotecan and bevacizumab correlated well with overall survival.[70] Early studies on breast cancer have also demonstrated that changes in FLT uptake during treatment predict clinical response, and multicenter trials for breast cancer are ongoing.[71,72] In patients with nonsmall cell lung cancer, a reduction in FLT uptake after 7 days of therapy with gefitinib was highly predictive of tumor response on CT and of progression-free survival.[73] This is a notable result, in that proliferation imaging was effective for predicting response to a biologically targeted agent that often has a cytostatic response when used as monotherapy.

However, some studies have reported less striking results. In lymphoma, treatment with rituximab did not result in an early change in FLT uptake, although it has been a highly effective agent in the clinic, and some data support its impact on cellular proliferation.[74] Some more recent studies suggest that FLT may be taken up in proliferating immune cells, and it is possible that the immune effect of rituximab, a monoclonal antibody, could confound assessment of response by FLT-PET.[75] Conversely, in some patients, tumor FLT uptake changed significantly in patients who did not go on to have a subsequent clinical response. For example, a study of patients with rectal cancer who received neoadjuvant chemoradiation revealed that FLT uptake was reduced significantly at day 14 in all patients, but there was no difference in uptake reduction for histopathologically responding versus nonresponding lesions, suggesting that inhibition of proliferation, although necessary, may not be sufficient for a favorable response in some tumor types or with some types of treatment.[76] In such a case, the decrease in FLT uptake in histopathologic nonresponders may be because of treatment-induced growth arrest rather than cell death. An

alternative hypothesis relates to the finding that FLT traces only the salvage pathway for incorporation of thymidine into DNA, whereas many gastrointestinal cancers rely heavily on the de novo pathway, which is not tracked by FLT.[60,61] These findings indicate some potential limitations of FLT for monitoring the response to treatment, and it is likely that the choice of approach for early assessment of therapeutic response will need to be matched to the cancer and treatment types under study. Also, there is one report of a temporary rise in FLT uptake in patients with lung cancer who were receiving chemoradiation.[77] Thus, FLT uptake may be influenced by factors other than proliferation, such as altered vascular permeability, perfusion, or uptake in proliferating inflammatory cells, and additional study is needed.

Other PET proliferation imaging probes have also been tested.[78] The thymidine analog (1-[2′-deoxy-2′-^{18}F-fluoro-beta-D-arabinofuranosyl]thymine) (FMAU) can be phosphorylated and subsequently incorporated into DNA. Because FMAU has minimal bone marrow uptake and urinary excretion, it is a promising agent for studying bone metastases and genitourinary malignancies.[79] Preliminary in vitro studies have indicated that FMAU uptake is proportional to the rate of tumor proliferation.[80] However, additional studies are needed to evaluate the ability of FMAU to serve as a PET imaging biomarker of cell proliferation. There have also been efforts to image proliferation using methods distinct from probes like FLT and FMAU, which rely on the thymidine salvage pathway for DNA synthesis. A promising example is the use of sigma-2 receptor binding agents to measure tumor proliferation.[81] Like FLT, sigma-2 ligand binding levels increase with increasing cellular proliferation; however, sigma-2 agents have the potential advantage that, unlike FLT, they also produce some uptake in quiescent (nonproliferating) but viable cells.[81] Promising early studies in humans motivate further work in this area of research.[82]

Imaging Hypoxia

Tumor hypoxia is a pathologic state in which tumor tissues lack enough oxygen for normal metabolism. In solid tumors, oxygen delivery to the tumor cells is frequently reduced or even abolished by a deteriorating diffusion geometry, severe structural abnormalities of tumor microvessels, and disturbed microcirculation.[83] These microregions of hypoxia are distributed heterogeneously within the tumor mass and may be located adjacent to regions with normal oxygen partial pressures. It is noteworthy that >50% of locally advanced solid tumors may contain hypoxic tissue areas, and the presence or absence of hypoxia cannot be predicted by clinical size, stage, grade, histology, or site.[84] In solid tumors, hypoxia is associated with restrained proliferation, differentiation, apoptosis, and necrosis. At the same time, hypoxia may promote tumor progression through mechanisms that enable tumor cells to overcome nutritive deficiency, escape from a hostile environment, and favor unrestricted growth.[85] Sustained hypoxia also may lead to cellular changes, resulting in a more clinically aggressive phenotype.[85] In addition, tumor hypoxia has been associated with treatment failure after radiotherapy and chemotherapy.[86,87] Thus, knowledge of the degree and extent of tumor hypoxia has the potential to play a significant role in staging and treatment planning for a wide variety of tumor types and, in certain patients, may help to direct patients to regional therapy and/or agents that are selective for hypoxic tissue.

Two major classes of PET radiotracers have been developed to image hypoxia: 2-nitroimidazoles, such as ^{18}F-fluoromisonidazole (FMISO), ^{18}F-EF5, and ^{18}F-fluoroetanidazole (FETA), and nucleoside conjugates, such as ^{18}F-fluoroazomycin arabinoside (FAZA) and ^{64}Cu-diacetyl-bis(N4-methylthiosemicarbazone) (Cu-ATSM). All of these agents undergo intracellular trapping at a rate inversely proportional to intracellular oxygen concentration.[85] In normal cells, the imaging agents are rapidly reoxidized and cleared, thus providing good demarcation between hypoxic and normoxic regions. Of the hypoxia imaging agents, FMISO has the largest body of preclinical validation studies and clinical experience, although the other PET hypoxia tracers also have been studied in patients.[88] Recent studies have demonstrated that tumor hypoxia measured by PET is predictive of patient outcome; patients with hypoxia by PET had considerably earlier relapse or progression.[89,90] However, not all studies demonstrate this correlation. For example, a study in patients with head and neck cancer demonstrated no correlation between hypoxia on PET imaging and patient outcome.[91] Thus, although PET hypoxia imaging has tremendous potential in treatment planning, more research is needed to better delineate the role of hypoxia imaging in cancer care.

Imaging Apoptosis

Programmed cell death, or apoptosis, is an essential component of normal human growth and development, immunoregulation and tissue homeostasis. It is generally accepted that effective therapy of tumors by radiation, chemotherapy, or both, leads to induction of apoptosis.[92]

Preclinical and clinical studies have shown that the detection of apoptosis can potentially be used to provide an early indication of the success of therapy.[93] Thus, several different classes of apoptotic imaging agents have been developed.

The first class of imaging agents targets phosphytidylserine residues that normally reside on the intracellular membrane surface but that are translocated to the extracellular surface during apoptosis. The single-photon emission CT (SPECT) agent technetium-99m (^{99m}Tc)-annexin V, a radiolabeled protein with nanomolar affinity to phosphytidylserine, is the most widely used imaging probe in this class. Although ^{99m}Tc-annexin V has a suboptimal biodistribution profile characterized by high background activity, including confounding uptake in the liver, multiple studies have demonstrated that ^{99m}Tc-annexin V is able to image apoptosis in vivo and to predict patient outcome after chemotherapy or radiation therapy.[94,95] However, more data are needed to support the ability of ^{99m}Tc-annexin V to predict long-term treatment outcomes. More recently, ^{18}F-annexin V has been synthesized, and it has an improved biodistribution profile and can be imaged using PET; preliminary studies of ^{18}F-annexin V have been done in animals but not in humans.[96]

A second class of imaging agents targets caspases, which are cysteine-aspartate proteases that play a pivotal role in the regulation of apoptosis. Two of the main imaging agents in this class are ^{18}F-ICMT-11 (a caspase-3-specific small molecule PET tracer based on the caspase inhibitor isatin) and ^{18}F-CP18 (a pentapeptide-based PET tracer that is a substrate of caspase-3). Both of these agents have demonstrated promise for the early detection of drug-induced tumor apoptosis in several animal models, and the biodistribution of both agents has been studied in humans.[97,98] However, to date, no clinical trials have evaluated the ability of these imaging agents to predict patient outcome.

A third class of imaging agents is thought to detect plasma membrane depolarization, although the exact mechanism has not yet been fully elucidated. The most notable of these imaging agents is the PET tracer ^{18}F-ML-10 (an ^{18}F-labeled small molecule malonic acid-based probe). A recent study of 10 patients with brain metastases who received whole-brain radiation therapy demonstrated a significant correlation between early changes in ^{18}F-ML-10 PET scans and size changes on MRI at 6 to 8 weeks after treatment.[99] Multicenter clinical trials are currently taking place to assess ^{18}F-ML-10 in multiple tumor types.[99]

One of the limitations of imaging apoptosis is related to its rapid evolution, which renders imaging of the transient apoptotic biomarkers particularly challenging.[100] In fact, in some patients, the ideal temporal window for imaging occurs between 6 and 24 hours after treatment.[101] Thus, concern has been expressed that the relatively small number of cells undergoing apoptosis at any one time and the small time window to have access to the biomarkers during the apoptotic process may limit the widespread use of apoptosis imaging.[102] However, these same considerations may provide an advantage for mechanistic studies of early response that are important in determining optimal timing in multiagent therapy.

Imaging Protein and Cell Membrane Metabolism

The process of protein synthesis in tumors is increased because of the uncontrolled and accelerated growth of cancer.[103] Consequently, the demand for amino acids—the building blocks of proteins—is increased. In this regard, studies have demonstrated that many types of tumor cells have significantly increased L-type amino acid transporter 1 (LAT1) expression, which is the major transporter of large neutral amino acids.[104] Thus, increased protein synthesis/LAT1 expression is an excellent target for tumor imaging. Although almost all of the amino acids have been radiolabeled, only a few have been used clinically as PET imaging agents. These include ^{11}C-methionine (MET), ^{18}F-fluoroethyl-tyrosine (FET), ^{18}F-fluoromethyl-tyrosine (FMT), 1-amino-3-^{18}F-fluorocyclobutane-1-carboxylic acid (FACBC), and 3,4-dihydroxy-6-^{18}F-fluoro-L-phenylalanine (FDOPA).

MET-PET is the most popular amino acid imaging modality in oncology, with over 300 basic scientific and clinical publications. MET-PET has been used primarily to image cerebral gliomas, and it has been used for initial diagnosis, differentiation of tumor recurrence from radiation necrosis, grading, prognostication, delineation of tumor extent, biopsy planning, surgical resection and radiotherapy planning, and assessment of response to therapy.[105] Because large neutral amino acids like MET are able to cross the blood-brain barrier and enter normal brain tissue, disruption of the blood-brain barrier (ie, contrast enhancement on CT or MRI) is not a prerequisite for intratumoral accumulation of these amino acids. Uptake of FLT, conversely, depends on blood-brain barrier damage, because transport across the normal blood-brain barrier is slow for thymidine. Thus, nonenhancing, low-grade gliomas can be observed with MET, but not with FLT.[106] MET-PET also has been used clinically to distinguish benign from malignant tissue in head and

neck cancer, melanoma, ovarian cancer, and other tumors.[107] One of the advantages of MET and other radiolabeled amino acids over FDG is their relatively low uptake in normal brain, which makes them more specific for tumor detection and better at tumor delineation and staging. In addition, amino acid radiotracers generally are affected less by inflammation compared with FDG, although tumor specificity is still not perfect.[108]

The short half-life of ^{11}C prevents the widespread use of MET-PET for tumor imaging, and awareness of this limitation has stimulated the development and evaluation of ^{18}F-labeled amino acids like FET, FMT, FACBC, and FDOPA. Several clinical studies with small numbers of patients have suggested that FMT is superior to FDG for the detection of musculoskeletal tumors, similar to FDG for the detection of head and neck tumors, and is superior to FDG for determining treatment response in lung cancer.[109,110] Conversely, small clinical studies that used FET indicated that it was generally worse than FDG for the detection of many tumor types, including head and neck cancer.[111,112] FET-PET did exhibit better specificity in several of the studies, raising the possibility that it may be better at differentiating tumor from inflammatory tissue. Also, when FET-PET was compared directly with MET-PET in 42 patients with gliomas or brain metastases, the 2 imaging agents provided comparable diagnostic information.[113] FDOPA-PET also was compared with MET-PET in patients with primary brain tumors or brain metastases and, similarly, yielded comparable diagnostic information.[114] FACBC has been studied primarily in prostate cancer, in which it had higher sensitivity for tumor detection compared with ^{111}In-capromab pendetide (Prostascint) and ^{11}C-choline.[115,116] In addition, FACBC has demonstrated increased uptake in papillary renal cell carcinoma, but not in clear cell carcinoma.[117] FACBC is especially notable for the lack of associated radioactivity in the urine, which allows for better evaluation of the genitourinary tract and pelvis.

Choline is a precursor of phosphatidylcholine, which is a major constituent of membrane lipids. Because both membrane lipid synthesis and protein synthesis are activated during cell proliferation, choline is consumed in large quantities by tumor cells.[118] Thus, ^{11}C-choline accumulation is significantly greater in malignant tumors than in benign lesions. Most reports of ^{11}C-choline PET imaging involve prostate cancer, although ^{11}C-choline uptake also is increased in a wide variety of other tumors.[119,120] Given its lack of radiotracer activity in the urine, ^{11}C-choline is well suited to evaluate pelvic malignancies.[119] In recent studies of patients with prostate cancer, ^{11}C-choline PET identified recurrent disease in 66% of patients with a mean prostate-specific antigen (PSA) level of 8.3 ng/mL, 28% of patients with a PSA level <1.5 ng/mL, and 21% of patients with a PSA level <0.5 ng/mL.[121,122] In addition, ^{11}C-choline PET demonstrated better sensitivity than MRI for lymph node metastases in prostate cancer.[123] More recently, ^{18}F-choline (FCH), which has the advantage of a much longer half-life compared with that of ^{11}C, has been developed. To date, studies of FCH have focused largely on prostate cancer, for which FCH has performed similarly to ^{11}C-choline.[124]

Imaging Tumor-Specific Agents

Although tracers for metabolism, proliferation, and hypoxia provide useful imaging of neoplasms, they are relatively nonspecific and are usually less useful for imaging tumors that have very low growth rates. Therefore, the development of tracers targeting intracellular and cell-surface receptors that are uniquely expressed or overexpressed in cancer cells is essential for the development and usefulness of clinical PET. Examples of radiotracers that target these tumor-specific biomarkers are outlined below.

Prostate-specific membrane antigen (PSMA) is a cell surface protein that is highly expressed in prostate carcinoma cells. Several radiotracers that target PSMA have been developed and studied preclinically. Recently, both ^{18}F-DCFBC (N-[N-([S]-1,3-dicarboxypropyl)carbamoyl]-4-^{18}F-fluorobenzyl-L-cysteine) and ^{68}Ga-PSMA have been studied in humans, and both reportedly were capable of detecting sites of metastatic prostate cancer.[125,126] In a subsequent, small clinical trial, ^{68}Ga-PSMA detected more lesions than ^{18}F-choline.[127]

Somatostatin receptors are overexpressed on neuroendocrine tumor cells. Imaging of this biomarker is currently accomplished using SPECT with ^{111}In-diethylenetriaminepentaacetic acid (DTPA)-octreotide; however, several new radiotracers have been developed that can be imaged using PET. Examples include ^{68}Ga-1,4,7,10-tetraazacyclododecane-1,4,7,10-tetraacetic acid (DOTA)-Tyr^3-octreotide (^{68}Ga-DOTA-TOC), ^{68}Ga-DOTA-1-Nal^3-octreotide (^{68}Ga-DOTA-NOC), and ^{68}Ga-DOTA-Tyr^3-octreotate (DOTA-TATE), all of which demonstrate better sensitivity than ^{111}In-DTPA-octreotide for neuroendocrine tumors, and all have the additional benefit of better resolution because they are imaged using PET.[128] Although all 3 radiotracers demonstrate variable affinity to somatostatin receptor subtypes, there is currently no evidence of a clinical impact from these differences; thus, there is no indication suggesting the preferential use of one compound over the others.[128]

In addition, there are several cancer therapies that target a specific receptor or enzyme in tumor cells. Current examples of specific targets (and examples of treatments directed at them) include the estrogen receptor (tamoxifen and letrozole), HER2 (trastuzumab), epidermal growth factor receptor (gefitinib), and angiogenesis (bevacizumab).[129] Measuring the target expression at each site of disease is a task for which PET is well suited. PET imaging can determine whether the target is expressed at all disease sites and can quantify the level of target expression at each site. Current examples of PET imaging to measure target expression include estrogen receptor imaging and androgen receptor imaging; HER2 imaging; imaging angiogenesis nonspecifically by measuring blood flow and by imaging specific components expressed in neovasculature; and measuring novel targets, such as matrix metalloproteinases.[130-135] In all of these cases, PET imaging has the potential to provide prognostic information and can help predict the likelihood that a patient will respond to a targeted chemotherapeutic agent. One of the major imaging agents in this class is ^{18}F-fluoroestradiol (FES), which has exhibited the most promise in quantifying the functional estrogen receptor status of primary or metastatic breast cancer.[136] Studies by Mortimer et al have demonstrated that a high level of FES uptake in advanced breast cancer predicts a greater likelihood of response to tamoxifen.[44] More recent studies report similar results for patients with recurrent or metastatic breast cancer who received a variety of hormonal agents.[137] These preliminary results demonstrate the exciting potential of PET imaging to help guide appropriate, individualized treatment for cancer, and they point the way for future clinical use.

Summary

PET is an established technique for cancer detection, and FDG continues to be the most widely used radiotracer for the staging and restaging of most tumors. However, many of the newer radiotracers described in this article will likely play a larger role in cancer care in the future and, along with FDG, will be used increasingly to determine a patient's prognosis, make decisions regarding treatment planning, and evaluate treatment response. In addition, new radiotracers will continue to be developed as diagnostic agents for tumors with minimal FDG uptake, such as prostate cancer and neuroendocrine tumors. Unfortunately, several barriers to the development and use of new radiotracers exist; these include a costly FDA approval process, relatively small profit potential (and, thus, little interest by the pharmaceutical industry in sponsoring clinical trials), as well as uncertain reimbursement by the US Centers for Medicare and Medicaid Services and by private insurers. Thus, future applications of PET for cancer imaging will need to rely on robust and reproducible quantitative data to validate the ability of PET to serve as an effective biomarker, and the passage of new radiotracers through the FDA and Centers for Medicare and Medicaid Services approval processes must be supported.

FUNDING SUPPORT

No specific funding was disclosed.

CONFLICT OF INTEREST DISCLOSURES

Dr. Pryma reports personal fees from IBA Molecular and a grant from Siemens Medical. Dr. Mankoff reports grants and personal fees from Siemens Medical and Phillips Medical, and he serves on the GE Medical advisory board.

REFERENCES

1. IMV Medical Information Division. 2012 PET Imaging Market Summary Report. Des Plaines, IL: IMV Medical Information Division; 2012.
2. Eubank WB, Mankoff DA, Schmiedl UP, et al. Imaging of oncologic patients: benefit of combined CT and FDG-PET in the diagnosis of malignancy. *AJR Am J Roentgenol*. 1998;171:1103-1110.
3. Shim SS, Lee KS, Kim BT, et al. Non-small cell lung cancer: prospective comparison of integrated FDG PET/CT and CT alone for preoperative staging. *Radiology*. 2005;236:1011-1019.
4. Sokoloff L, Reivich M, Kennedy C, et al. The [^{14}C]deoxyglucose method for the measurement of local cerebral glucose utilization: theory, procedure, and normal values in the conscious and anesthetized albino rat. *J Neurochem*. 1977;28:897-916.
5. Smith TA. Mammalian hexokinases and their abnormal expression in cancer. *Br J Biomed Sci*. 2000;57:170-178.
6. Phelps ME, Huang SC, Hoffman EJ, Selin C, Sokoloff L, Kuhl DE. Tomographic measurement of local cerebral glucose metabolic rate in humans with (F-18)2-fluoro-2-deoxy-D-glucose: validation of method. *Ann Neurol*. 1979;6:371-388.
7. Shankar LK, Hoffman JM, Bacharach S, et al. Consensus recommendations for the use of ^{18}F-FDG-PET as an indicator of therapeutic response in patients in National Cancer Institute Trials. *J Nucl Med*. 2006;47:1059-1066.
8. Huang SC. Anatomy of SUV. *Standardized uptake value. Nucl Med Biol*. 2000;27:643-646.
9. Krohn KA, Mankoff DA, Muzi M, Link JM, Spence AM. True tracers: comparing FDG with glucose and FLT with thymidine. *Nucl Med Biol*. 2005;32:663-671.
10. Paquet N, Albert A, Foidart J, Hustinx R. Within-patient variability of (18)F-FDG: standardized uptake values in normal tissues. *J Nucl Med*. 2004;45:784-788.
11. Weber WA, Ziegler SI, Thodtmann R, Hanauske AR, Schwaiger M. Reproducibility of metabolic measurements in malignant tumors using FDG PET. *J Nucl Med*. 1999;40:1771-1777.
12. Warburg O. Metabolism of Tumors. London, UK: Constable and Company; 1930.
13. Mathupala SP, Rempel A, Pedersen PL. Aberrant glycolytic metabolism of cancer cells: a remarkable coordination of genetic, transcriptional, post-translational, and mutational events that lead to a critical role for type II hexokinase. *J Bioenerg Biomembr*. 1997;29:339-343.
14. Szablewski L. Expression of glucose transporters in cancers. *Biochim Biophys Acta*. 2013;1835:164-169.

15. Di Chiro G. Positron emission tomography using [^{18}F] fluorodeoxyglucose in brain tumors. A powerful diagnostic and prognostic tool. *Invest Radiol*. 1987;22:360-371.
16. Hillner BE, Siegel BA, Hanna L, et al. Impact of ^{18}F-FDG PET used after initial treatment of cancer: comparison of the National Oncologic PET Registry 2006 and 2009 cohorts. *J Nucl Med*. 2012;53:831-837.
17. Kelloff GJ, Hoffman JM, Johnson B, et al. Progress and promise of FDG-PET imaging for cancer patient management and oncologic drug development. *Clin Cancer Res*. 2005;11:2785-2808.
18. Cuaron J, Dunphy M, Rimner A. Role of FDG-PET scans in staging, response assessment, and follow-up care for non-small cell lung cancer. *Front Oncol*. 2012;2:208.
19. Eubank WB, Mankoff DA. Current and future uses of positron emission tomography in breast cancer imaging. *Semin Nucl Med*. 2004;34:224-240.
20. Macapinlac HA. FDG PET and PET/CT imaging in lymphoma and melanoma. *Cancer J*. 2004;10:262-270.
21. Hoh CK, Seltzer MA, Franklin J, deKernion JB, Phelps ME, Belldegrun A. Positron emission tomography in urological oncology. *J Urol*. 1998;159:347-356.
22. Khan MA, Combs CS, Brunt EM, et al. Positron emission tomography scanning in the evaluation of hepatocellular carcinoma. *J Hepatol*. 2000;32:792-797.
23. Bos R, van Der Hoeven JJ, van Der Wall E, et al. Biologic correlates of (18)fluorodeoxyglucose uptake in human breast cancer measured by positron emission tomography. *J Clin Oncol*. 2002;20:379-387.
24. Buerkle A, Weber WA. Imaging of tumor glucose utilization with positron emission tomography. *Cancer Metastasis Rev*. 2008;27:545-554.
25. Morris MJ, Akhurst T, Osman I, et al. Fluorinated deoxyglucose positron emission tomography imaging in progressive metastatic prostate cancer. *Urology*. 2002;59:913-918.
26. Wang W, Larson SM, Tuttle RM, et al. Resistance of [^{18}F]-fluorodeoxyglucose-avid metastatic thyroid cancer lesions to treatment with high-dose radioactive iodine. *Thyroid*. 2001;11:1169-1175.
27. Minn H, Soini I. [^{18}F]fluorodeoxyglucose scintigraphy in diagnosis and follow up of treatment in advanced breast cancer. *Eur J Nucl Med*. 1989;15:61-66.
28. Wahl RL, Zasadny K, Helvie M, Hutchins GD, Weber B, Cody R. Metabolic monitoring of breast cancer chemohormonotherapy using positron emission tomography: initial evaluation. *J Clin Oncol*. 1993;11:2101-2111.
29. Krause BJ, Herrmann K, Wieder H, zum Buschenfelde CM. ^{18}F-FDG PET and ^{18}F-FDG PET/CT for assessing response to therapy in esophageal cancer. *J Nucl Med*. 2009;50(suppl 1):89S-96S.
30. Hutchings M, Loft A, Hansen M, et al. FDG-PET after two cycles of chemotherapy predicts treatment failure and progression-free survival in Hodgkin lymphoma. *Blood*. 2006;107:52-59.
31. Mankoff DA, Dunnwald LK, Gralow JR, et al. Changes in blood flow and metabolism in locally advanced breast cancer treated with neoadjuvant chemotherapy. *J Nucl Med*. 2003;44:1806-1814.
32. Hillner BE, Siegel BA, Shields AF, et al. The impact of positron emission tomography (PET) on expected management during cancer treatment: findings of the National Oncologic PET Registry. *Cancer*. 2009;115:410-418.
33. Ott K, Weber WA, Lordick F, et al. Metabolic imaging predicts response, survival, and recurrence in adenocarcinomas of the esophagogastric junction. *J Clin Oncol*. 2006;24:4692-4698.
34. Romer W, Hanauske AR, Ziegler S, et al. Positron emission tomography in non-Hodgkin's lymphoma: assessment of chemotherapy with fluorodeoxyglucose. *Blood*. 1998;91:4464-4471.
35. Smith IC, Welch AE, Hutcheon AW, et al. Positron emission tomography using [(18)F]-fluorodeoxy-D-glucose to predict the pathologic response of breast cancer to primary chemotherapy. *J Clin Oncol*. 2000;18:1676-1688.
36. Yamane T, Daimaru O, Ito S, Yoshiya K, Nagata T, Uchida H. Decreased ^{18}F-FDG uptake 1 day after initiation of chemotherapy for malignant lymphomas. *J Nucl Med*. 2004;45:1838-1842.
37. Cullinane C, Dorow DS, Kansara M, et al. An in vivo tumor model exploiting metabolic response as a biomarker for targeted drug development. *Cancer Res*. 2005;65:9633-9636.
38. Shinto A, Nair N, Dutt A, Baghel NS. Early response assessment in gastrointestinal stromal tumors with FDG PET scan 24 hours after a single dose of imatinib. *Clin Nucl Med*. 2008;33:486-487.
39. Stroobants S, Goeminne J, Seegers M, et al. ^{18}FDG-Positron emission tomography for the early prediction of response in advanced soft tissue sarcoma treated with imatinib mesylate (Glivec). *Eur J Cancer*. 2003;39:2012-2020.
40. Su H, Bodenstein C, Dumont RA, et al. Monitoring tumor glucose utilization by positron emission tomography for the prediction of treatment response to epidermal growth factor receptor kinase inhibitors. *Clin Cancer Res*. 2006;12:5659-5667.
41. Linden HM, Krohn KA, Livingston RB, Mankoff DA. Monitoring targeted therapy: is fluorodeoxyglucose uptake a marker of early response? *Clin Cancer Res*. 2006;12:5608-5610.
42. Demetri GD, Heinrich MC, Fletcher JA, et al. Molecular target modulation, imaging, and clinical evaluation of gastrointestinal stromal tumor patients treated with sunitinib malate after imatinib failure. *Clin Cancer Res*. 2009;15:5902-5909.
43. Van den Abbeele AD. The lessons of GIST—PET and PET/CT: a new paradigm for imaging. *Oncologist*. 2008;13(suppl 2):8-13.
44. Mortimer JE, Dehdashti F, Siegel BA, Trinkaus K, Katzenellenbogen JA, Welch MJ. Metabolic flare: indicator of hormone responsiveness in advanced breast cancer. *J Clin Oncol*. 2001; 19:2797-2803.
45. Hicks RJ. The role of PET in monitoring therapy. *Cancer Imaging*. 2005;5:51-57.
46. Spence AM, Muzi M, Graham MM, et al. 2-[(18)F]Fluoro-2-deoxyglucose and glucose uptake in malignant gliomas before and after radiotherapy: correlation with outcome. *Clin Cancer Res*. 2002;8: 971-979.
47. Young H, Baum R, Cremerius U, et al. Measurement of clinical and subclinical tumour response using [^{18}F]-fluorodeoxyglucose and positron emission tomography: review and 1999 EORTC recommendations. European Organization for Research and Treatment of Cancer (EORTC) PET Study Group. *Eur J Cancer*. 1999; 35:1773-1782.
48. Wahl RL, Jacene H, Kasamon Y, Lodge MA. From RECIST to PERCIST: evolving considerations for PET response criteria in solid tumors. *J Nucl Med*. 2009;50(suppl 1):122S-150S.
49. Weber WA. Positron emission tomography as an imaging biomarker. *J Clin Oncol*. 2006;24:3282-3292.
50. Kubota R, Yamada S, Kubota K, Ishiwata K, Tamahashi N, Ido T. Intratumoral distribution of fluorine-18-fluorodeoxyglucose in vivo: high accumulation in macrophages and granulation tissues studied by microautoradiography. *J Nucl Med*. 1992;33:1972-1980.
51. Buck AK, Halter G, Schirrmeister H, et al. Imaging proliferation in lung tumors with PET: ^{18}F-FLT versus ^{18}F-FDG. *J Nucl Med*. 2003;44:1426-1431.
52. Eary JF, O'Sullivan F, Powitan Y, et al. Sarcoma tumor FDG uptake measured by PET and patient outcome: a retrospective analysis. *Eur J Nucl Med Mol Imaging*. 2002;29:1149-1154.
53. Robbins RJ, Wan Q, Grewal RK, et al. Real-time prognosis for metastatic thyroid carcinoma based on 2-[^{18}F]fluoro-2-deoxy-D-glucose-positron emission tomography scanning. *J Clin Endocrinol Metab*. 2006;91:498-505.
54. Fulham MJ, Melisi JW, Nishimiya J, Dwyer AJ, Di Chiro G. Neuroimaging of juvenile pilocytic astrocytomas: an enigma. *Radiology*. 1993;189:221-225.
55. Kole AC, Nieweg OE, Hoekstra HJ, van Horn JR, Koops HS, Vaalburg W. Fluorine-18-fluorodeoxyglucose assessment of glucose metabolism in bone tumors. *J Nucl Med*. 1998;39:810-815.
56. Uchida Y, Minoshima S, Kawata T, et al. Diagnostic value of FDG PET and salivary gland scintigraphy for parotid tumors. *Clin Nucl Med*. 2005;30:170-176.
57. Hanahan D, Weinberg RA. Hallmarks of cancer: the next generation. *Cell*. 2011;144:646-674.
58. Weber WA. Monitoring tumor response to therapy with ^{18}F-FLT PET. *J Nucl Med*. 2010;51:841-844.
59. Troost EG, Bussink J, Hoffmann AL, Boerman OC, Oyen WJ, Kaanders JH. ^{18}F-FLT PET/CT for early response monitoring and dose escalation in oropharyngeal tumors. *J Nucl Med*. 2010;51:866-874.

60. Barwick T, Bencherif B, Mountz JM, Avril N. Molecular PET and PET/CT imaging of tumour cell proliferation using F-18 fluoro-L-thymidine: a comprehensive evaluation. *Nucl Med Commun*. 2009; 30:908-917.
61. Mankoff DA, Shields AF, Krohn KA. PET imaging of cellular proliferation. *Radiol Clin North Am*. 2005;43:153-167.
62. Shields AF, Grierson JR, Dohmen BM, et al. Imaging proliferation in vivo with [F-18]FLT and positron emission tomography. *Nat Med*. 1998;4:1334-1336.
63. Grierson JR, Shields AF. Radiosynthesis of 3′-deoxy-3′-[(18)F]fluorothymidine: [(18)F]FLT for imaging of cellular proliferation in vivo. *Nucl Med Biol*. 2000;27:143-156.
64. Paproski RJ, Ng AM, Yao SY, Graham K, Young JD, Cass CE. The role of human nucleoside transporters in uptake of 3′-deoxy-3′-fluorothymidine. *Mol Pharmacol*. 2008;74:1372-1380.
65. Chalkidou A, Landau DB, Odell EW, Cornelius VR, O'Doherty MJ, Marsden PK. Correlation between Ki-67 immunohistochemistry and ^{18}F-fluorothymidine uptake in patients with cancer: a systematic review and meta-analysis. *Eur J Cancer*. 2012;48:3499-3513.
66. Troost EG, Vogel WV, Merkx MA, et al. ^{18}F-FLT PET does not discriminate between reactive and metastatic lymph nodes in primary head and neck cancer patients. *J Nucl Med*. 2007;48:726-735.
67. Mankoff D. Imaging studies in anticancer drug development. In: Garrett-Mayer E, ed. Principles of Anticancer Drug Development: New York: Springer; 2011:275-302.
68. Apisarnthanarax S, Alauddin MM, Mourtada F, et al. Early detection of chemoradioresponse in esophageal carcinoma by 3′-deoxy-3′-3H-fluorothymidine using preclinical tumor models. *Clin Cancer Res*. 2006;12:4590-4597.
69. Ullrich RT, Zander T, Neumaier B, et al. Early detection of erlotinib treatment response in NSCLC by 3′-deoxy-3′-[^{18}F]-fluoro-L-thymidine ([^{18}F]FLT) positron emission tomography (PET). *PLoS One*. 2008;3:e3908.
70. Wardak M, Schiepers C, Dahlbom M, et al. Discriminant analysis of (18)F-fluorothymidine kinetic parameters to predict survival in patients with recurrent high-grade glioma. *Clin Cancer Res*. 2011; 17:6553-6562.
71. Kenny L, Coombes RC, Vigushin DM, Al-Nahhas A, Shousha S, Aboagye EO. Imaging early changes in proliferation at 1 week post chemotherapy: a pilot study in breast cancer patients with 3′-deoxy-3′-[^{18}F]fluorothymidine positron emission tomography. *Eur J Nucl Med Mol Imaging*. 2007;34:1339-1347.
72. Jolles PR, Kostakoglu L, Bear HD, et al. ACRIN 6688 phase II study of fluorine-18 3′-deoxy-3′ fluorothymidine (FLT) in invasive breast cancer. *J Clin Oncol*. 2011;29S. Abstract TPS125.
73. Sohn HJ, Yang YJ, Ryu JS, et al. [^{18}F]Fluorothymidine positron emission tomography before and 7 days after gefitinib treatment predicts response in patients with advanced adenocarcinoma of the lung. *Clin Cancer Res*. 2008;14:7423-7429.
74. Herrmann K, Wieder HA, Buck AK, et al. Early response assessment using 3′-deoxy-3′-[^{18}F]fluorothymidine-positron emission tomography in high-grade non-Hodgkin's lymphoma. *Clin Cancer Res*. 2007;13:3552-3558.
75. Aarntzen EH, Srinivas M, De Wilt JH, et al. Early identification of antigen-specific immune responses in vivo by [^{18}F]-labeled 3′-fluoro-3′-deoxy-thymidine ([^{18}F]FLT) PET imaging. *Proc Natl Acad Sci U S A*. 2011;108:18396-18399.
76. Wieder HA, Geinitz H, Rosenberg R, et al. PET imaging with [^{18}F]3′-deoxy-3′-fluorothymidine for prediction of response to neoadjuvant treatment in patients with rectal cancer. *Eur J Nucl Med Mol Imaging*. 2007;34:878-883.
77. Everitt S, Hicks RJ, Ball D, et al. Imaging cellular proliferation during chemo-radiotherapy: a pilot study of serial ^{18}F-FLT positron emission tomography/computed tomography imaging for non-small-cell lung cancer. *Int J Radiat Oncol Biol Phys*. 2009;75:1098-1104.
78. Bading JR, Shields AF. Imaging of cell proliferation: status and prospects. *J Nucl Med*. 2008;49(suppl 2):64S-80S.
79. Sun H, Sloan A, Mangner TJ, et al. Imaging DNA synthesis with [^{18}F]FMAU and positron emission tomography in patients with cancer. *Eur J Nucl Med Mol Imaging*. 2005;32:15-22.
80. Nishii R, Volgin AY, Mawlawi O, et al. Evaluation of 2′-deoxy-2′-[^{18}F]fluoro-5-methyl-1-beta-L-arabinofuranosyluracil ([^{18}F]-L-FMAU) as a PET imaging agent for cellular proliferation: comparison with [^{18}F]-D-FMAU and [^{18}F]FLT. *Eur J Nucl Med Mol Imaging*. 2008; 35:990-998.
81. Sai KK, Jones LA, Mach RH. Development of (18)F-labeled PET probes for imaging cell proliferation. *Curr Top Med Chem*. 2013; 13:892-908.
82. Dehdashti F, Laforest R, Gao F, et al. Assessment of cellular proliferation in tumors by PET using ^{18}F-ISO-1. *J Nucl Med*. 2013;54: 350-357.
83. Vaupel P, Kallinowski F, Okunieff P. Blood flow, oxygen and nutrient supply, and metabolic microenvironment of human tumors: a review. *Cancer Res*. 1989;49:6449-6465.
84. Vaupel P, Mayer A. Hypoxia in cancer: significance and impact on clinical outcome. *Cancer Metastasis Rev*. 2007;26:225-239.
85. Sun X, Niu G, Chan N, Shen B, Chen X. Tumor hypoxia imaging. *Mol Imaging Biol*. 2011;13:399-410.
86. Matthews NE, Adams MA, Maxwell LR, Gofton TE, Graham CH. Nitric oxide-mediated regulation of chemosensitivity in cancer cells. *J Natl Cancer Inst*. 2001;93:1879-1885.
87. Nordsmark M, Bentzen SM, Rudat V, et al. Prognostic value of tumor oxygenation in 397 head and neck tumors after primary radiation therapy. *An international multi-center study. Radiother Oncol*. 2005;77:18-24.
88. Rajendran JG, Krohn KA. Imaging hypoxia and angiogenesis in tumors. *Radiol Clin North Am*. 2005;43:169-187.
89. Dehdashti F, Grigsby PW, Lewis JS, Laforest R, Siegel BA, Welch MJ. Assessing tumor hypoxia in cervical cancer by PET with ^{60}Cu-labeled diacetyl-bis(N4-methylthiosemicarbazone). *J Nucl Med*. 2008;49:201-205.
90. Rischin D, Hicks RJ, Fisher R, et al. Prognostic significance of [^{18}F]-misonidazole positron emission tomography-detected tumor hypoxia in patients with advanced head and neck cancer randomly assigned to chemoradiation with or without tirapazamine: a substudy of Trans-Tasman Radiation Oncology Group Study 98.02. *J Clin Oncol*. 2006;24:2098-2104.
91. Lee N, Nehmeh S, Schoder H, et al. Prospective trial incorporating pre-/mid-treatment [^{18}F]-misonidazole positron emission tomography for head-and-neck cancer patients undergoing concurrent chemoradiotherapy. *Int J Radiat Oncol Biol Phys*. 2009;75:101-108.
92. Baskar R, Lee KA, Yeo R, Yeoh KW. Cancer and radiation therapy: current advances and future directions. *Int J Med Sci*. 2012;9: 193-199.
93. Buchholz TA, Davis DW, McConkey DJ, et al. Chemotherapy-induced apoptosis and Bcl-2 levels correlate with breast cancer response to chemotherapy. *Cancer J*. 2003;9:33-41.
94. Kartachova M, van Zandwijk N, Burgers S, van Tinteren H, Verheij M, Valdes Olmos RA. Prognostic significance of ^{99m}Tc Hynic-rh-annexin V scintigraphy during platinum-based chemotherapy in advanced lung cancer. *J Clin Oncol*. 2007;25:2534-2539.
95. Loose D, Vermeersch H, De Vos F, Deron P, Slegers G, Van de Wiele C. Prognostic value of ^{99m}Tc-HYNIC annexin-V imaging in squamous cell carcinoma of the head and neck. *Eur J Nucl Med Mol Imaging*. 2008;35:47-52.
96. Murakami Y, Takamatsu H, Taki J, et al. ^{18}F-labelled annexin V: a PET tracer for apoptosis imaging. *Eur J Nucl Med Mol Imaging*. 2004;31:469-474.
97. Challapalli A, Kenny LM, Hallett WA, et al. ^{18}F-ICMT-11, a caspase-3-specific PET tracer for apoptosis: biodistribution and radiation dosimetry. *J Nucl Med*. 2013;54:1551-1556.
98. Doss M, Kolb HC, Walsh JC, et al. Biodistribution and radiation dosimetry of ^{18}F-CP-18, a potential apoptosis imaging agent, as determined from PET/CT scans in healthy volunteers. *J Nucl Med*. 2013;54:2087-2092.
99. Allen AM, Ben-Ami M, Reshef A, et al. Assessment of response of brain metastases to radiotherapy by PET imaging of apoptosis with (18)F-ML-10. *Eur J Nucl Med Mol Imaging*. 2012;39:1400-1408.
100. Neves AA, Brindle KM. Imaging cell death. *J Nucl Med*. 2014;55: 1-4.

101. Nguyen QD, Lavdas I, Gubbins J, et al. Temporal and spatial evolution of therapy-induced tumor apoptosis detected by caspase-3-selective molecular imaging. *Clin Cancer Res*. 2013;19:3914-3924.
102. Mandl SJ, Mari C, Edinger M, et al. Multi-modality imaging identifies key times for annexin V imaging as an early predictor of therapeutic outcome. *Mol Imaging*. 2004;3:1-8.
103. Dolfi SC, Chan LL, Qiu J, et al. The metabolic demands of cancer cells are coupled to their size and protein synthesis rates. *Cancer Metab*. 2013;1:20.
104. Yanagida O, Kanai Y, Chairoungdua A, et al. Human L-type amino acid transporter 1 (LAT1): characterization of function and expression in tumor cell lines. *Biochim Biophys Acta*. 2001;1514: 291-302.
105. Singhal T, Narayanan TK, Jain V, Mukherjee J, Mantil J. ^{11}C-L-methionine positron emission tomography in the clinical management of cerebral gliomas. *Mol Imaging Biol*. 2008;10:1-18.
106. Langen K-J, Galldiks N. PET Imaging of Brain Tumors: Berlin; Springer; 2013.
107. Inoue T, Kim EE, Wong FC, et al. Comparison of fluorine-18-fluorodeoxyglucose and carbon-11-methionine PET in detection of malignant tumors. *J Nucl Med*. 1996;37:1472-1476.
108. Kubota R, Kubota K, Yamada S, et al. Methionine uptake by tumor tissue: a microautoradiographic comparison with FDG. *J Nucl Med*. 1995;36:484-492.
109. Miyakubo M, Oriuchi N, Tsushima Y, et al. Diagnosis of maxillofacial tumor with L-3-[^{18}F]-fluoro-alpha-methyltyrosine (FMT) PET: a comparative study with FDG-PET. *Ann Nucl Med*. 2007; 21:129-135.
110. Kaira K, Oriuchi N, Yanagitani N, et al. Assessment of therapy response in lung cancer with (18)F-alpha-methyl tyrosine PET. *AJR Am J Roentgenol*. 2010;195:1204-1211.
111. Pauleit D, Stoffels G, Schaden W, et al. PET with O-(2-^{18}F-fluoroethyl)-L-tyrosine in peripheral tumors: first clinical results. *J Nucl Med*. 2005;46:411-416.
112. Haerle SK, Fischer DR, Schmid DT, Ahmad N, Huber GF, Buck A. ^{18}F-FET PET/CT in advanced head and neck squamous cell carcinoma: an intra-individual comparison with ^{18}F-FDG PET/CT. *Mol Imaging Biol*. 2011;13:1036-1042.
113. Grosu AL, Astner ST, Riedel E, et al. An interindividual comparison of O-(2-[^{18}F]fluoroethyl)-L-tyrosine (FET)- and L-[methyl-^{11}C]methionine (MET)-PET in patients with brain gliomas and metastases. *Int J Radiat Oncol Biol Phys*. 2011;81:1049-1058.
114. Becherer A, Karanikas G, Szabo M, et al. Brain tumour imaging with PET: a comparison between [^{18}F]fluorodopa and [^{11}C]methionine. *Eur J Nucl Med Mol Imaging*. 2003;30:1561-1567.
115. Schuster DM, Nieh PT, Jani AB, et al. Anti-3-[(18)F]FACBC positron emission tomography-computerized tomography and (111)In-capromab pendetide single photon emission computerized tomography-computerized tomography in recurrent prostate carcinoma: results of a prospective clinical trial. *J Urol*. 2014;191:1446-1453.
116. Nanni C, Schiavina R, Brunocilla E, et al. ^{18}F-FACBC compared with ^{11}C-choline PET/CT in patients with biochemical relapse after radical prostatectomy: a prospective study in 28 patients. *Clin Genitourin Cancer*. 2014;12:106-110.
117. Schuster DM, Nye JA, Nieh PT, et al. Initial experience with the radiotracer anti-1-amino-3-[^{18}F]fluorocyclobutane-1-carboxylic acid (anti-[^{18}F]FACBC) with PET in renal carcinoma. *Mol Imaging Biol*. 2009;11:434-438.
118. Yoshimoto M, Waki A, Obata A, Furukawa T, Yonekura Y, Fujibayashi Y. Radiolabeled choline as a proliferation marker: comparison with radiolabeled acetate. *Nucl Med Biol*. 2004;31:859-865.
119. Tian M, Zhang H, Oriuchi N, Higuchi T, Endo K. Comparison of ^{11}C-choline PET and FDG PET for the differential diagnosis of malignant tumors. *Eur J Nucl Med Mol Imaging*. 2004;31:1064-1072.
120. Scher B, Seitz M, Albinger W, et al. Value of ^{11}C-choline PET and PET/CT in patients with suspected prostate cancer. *Eur J Nucl Med Mol Imaging*. 2007;34:45-53.
121. Ceci F, Castellucci P, Mamede M, et al. (11)C-Choline PET/CT in patients with hormone-resistant prostate cancer showing biochemical relapse after radical prostatectomy. *Eur J Nucl Med Mol Imaging*. 2013;40:149-155.
122. Mamede M, Ceci F, Castellucci P, et al. The role of ^{11}C-choline PET imaging in the early detection of recurrence in surgically treated prostate cancer patients with very low PSA level <0.5 ng/mL. *Clin Nucl Med*. 2013;38:e342-e345.
123. Contractor K, Challapalli A, Barwick T, et al. Use of [^{11}C]choline PET-CT as a noninvasive method for detecting pelvic lymph node status from prostate cancer and relationship with choline kinase expression. *Clin Cancer Res*. 2011;17:7673-7683.
124. Marzola MC, Chondrogiannis S, Ferretti A, et al. Role of ^{18}F-choline PET/CT in biochemically relapsed prostate cancer after radical prostatectomy: correlation with trigger PSA, PSA velocity, PSA doubling time, and metastatic distribution. *Clin Nucl Med*. 2013;38:e26-e32.
125. Afshar-Oromieh A, Malcher A, Eder M, et al. PET imaging with a [^{68}Ga]gallium-labelled PSMA ligand for the diagnosis of prostate cancer: biodistribution in humans and first evaluation of tumour lesions. *Eur J Nucl Med Mol Imaging*. 2013;40:486-495.
126. Cho SY, Gage KL, Mease RC, et al. Biodistribution, tumor detection, and radiation dosimetry of ^{18}F-DCFBC, a low-molecular-weight inhibitor of prostate-specific membrane antigen, in patients with metastatic prostate cancer. *J Nucl Med*. 2012;53:1883-1891.
127. Afshar-Oromieh A, Zechmann CM, Malcher A, et al. Comparison of PET imaging with a (68)Ga-labelled PSMA ligand and (18)F-choline-based PET/CT for the diagnosis of recurrent prostate cancer. *Eur J Nucl Med Mol Imaging*. 2014;41:11-20.
128. Ambrosini V, Campana D, Tomassetti P, Fanti S. (68)Ga-labelled peptides for diagnosis of gastroenteropancreatic NET. *Eur J Nucl Med Mol Imaging*. 2012;39(suppl 1):S52-S60.
129. Kaklamani V, O'Regan RM. New targeted therapies in breast cancer. *Semin Oncol*. 2004;31:20-25.
130. Dehdashti F, Mortimer JE, Siegel BA, et al. Positron tomographic assessment of estrogen receptors in breast cancer: comparison with FDG-PET and in vitro receptor assays. *J Nucl Med*. 1995;36:1766-1774.
131. Larson SM, Morris M, Gunther I, et al. Tumor localization of 16beta-^{18}F-fluoro-5alpha-dihydrotestosterone versus ^{18}F-FDG in patients with progressive, metastatic prostate cancer. *J Nucl Med*. 2004;45:366-373.
132. Dijkers EC, Oude Munnink TH, Kosterink JG, et al. Biodistribution of ^{89}Zr-trastuzumab and PET imaging of HER2-positive lesions in patients with metastatic breast cancer. *Clin Pharmacol Ther*. 2010;87:586-592.
133. Mankoff DA, Dunnwald LK, Gralow JR, et al. Blood flow and metabolism in locally advanced breast cancer: relationship to response to therapy. *J Nucl Med*. 2002;43:500-509.
134. Beer AJ, Haubner R, Sarbia M, et al. Positron emission tomography using [^{18}F]Galacto-RGD identifies the level of integrin alpha(v)beta3 expression in man. *Clin Cancer Res*. 2006;12:3942-3949.
135. Matusiak N, van Waarde A, Bischoff R, et al. Probes for non-invasive matrix metalloproteinase-targeted imaging with PET and SPECT. *Curr Pharm Des*. 2013;19:4647-4672.
136. Katzenellenbogen JA, Welch MJ, Dehdashti F. The development of estrogen and progestin radiopharmaceuticals for imaging breast cancer. *Anticancer Res*. 1997;17:1573-1576.
137. Linden HM, Stekhova SA, Link JM, et al. Quantitative fluoroestradiol positron emission tomography imaging predicts response to endocrine treatment in breast cancer. *J Clin Oncol*. 2006;24:2793-2799.